Journal of Applied Polymer Science

Thermoplastic Polyurethane Composites Prepared from Mechanochemically Activated Waste Cotton Fabric and Reclaimed Polyurethane Foam

Mengya Wang, Xinxing Zhang, Wei Zhang, Dong Tian, Canhui Lu
State Key Laboratory of Polymer Materials Engineering, Polymer Research Institute of Sichuan University, Chengdu 610065, China
Correspondence to: C. Lu (E-mail: canhuilu@263.net)

ABSTRACT: In this study, thermoplastic polyurethane (PU) composites were successfully prepared from waste cotton fabric (WCF) and reclaimed PU foam derived from the shoe manufacturing industry through melt mixing. A pan-mill-type mechanochemical reactor made in our laboratory was applied to determine the mechanochemical activation of WCF. The intramolecular and intermolecular hydrogen bonds of WCF could be broken up through pan milling because of the fairly strong shearing and squeezing forces. Moreover, the simultaneous reduction of particle size and the large increment of the specific surface area of pan-milled WCF benefitted its dispersion and the interfacial adhesion with the PU matrix. Mechanochemically activated WCF could be used as a low cost but effective functional additive to enhance the melt processability and mechanical properties of PU/WCF composites. With the addition of 75-phr WCF, the heat shrinkage of the melt-reprocessed PU decreased sharply from its original 11.4 to 0.3%. Meanwhile, the tensile strength of the composites was enhanced from 10.3 to 23.2 MPa. © 2012 Wiley Periodicals, Inc. J. Appl. Polym. Sci. 128: 3555–3563, 2013

KEYWORDS: composites; fibers; mechanical properties; polyurethanes; recycling

Received 4 May 2012; accepted 26 July 2012; published online 28 September 2012
DOI: 10.1002/app.38402

INTRODUCTION

Nowadays, polyurethane (PU) foams are used extensively as cushion materials because of their superior physical properties (e.g., high tensile strength, abrasion and tear resistance, low-temperature flexibility, oil and solvent resistance, paintability) and high versatility.[1,2] A considerable amount of PU foams are used in footwear (shoe soles). With the increasing quantity of PU wastes, the recycling of PU has become an urgent and important task. The methods used to recycle postused PU foams include mechanical recycling, recycling back to chemical feedstock, and recovery of energy. In the mechanical recycling process, PU foam was smashed into a fine powder and used as a filler for polymer and concrete materials.[3,4] However, this usually results in the deterioration of the mechanical properties of the obtained composites. Numerous studies on the chemical recycling of PU foams, such as through hydrolysis,[5] glycolysis,[6] aminoalcoholysis,[7] and methanolysis,[8] have been described in the literature. More recently, the degradation of PU by microorganisms was realized.[9] However, the difficulty of purifying the degraded products limits the large-scale industrial application of chemical recycling technology. On the other hand, the incineration process[10] for energy recycling is inevitably accompanied by the emission of toxic gases; this further aggravates environmental pollution. Therefore, there is still a challenge to develop a cost-effective method for the recycling of PU foams.

Waste cotton fabric (WCF), which is derived from used clothes and surplus from textile industries, represents another type of environmental problem. Nowadays, most WCF is landfilled or incinerated.[11] Efficient technology for the recycling of WCF is still under development.[12–14] WCF is neither meltable nor soluble in most common solvents because of its large amount of intramolecular and intermolecular hydrogen bonds and its high degree of crystallinity in structure, which destroys its processability.[15]

The aim of this study was to prepare thermoplastic composites from reclaimed PU foam and WCF and, thereby, to provide a cost-effective technology for recycling these two waste polymers simultaneously. WCF was pretreated by a self-designed pan-mill-type mechanochemical reactor to obtain a cellulose ultrafine powder and break up the hydrogen bonds in the cellulose. The pan-mill-type mechanochemical reactor was a novel pulverizing instrument.[16–22] The milled materials suffered from strong pressures and shear forces because of the space changes in the unit cells and the complex motion in both the circular and

radial directions. While undergoing stress, the polymer bonds were distorted, and the bond angles and distance were extended. When the imposed stress was beyond the chemical bonding energy, bond rupture occurred.[23] Our previous studies[24,25] confirmed that the hydrogen bonds in cellulose could be effectively broken up to expose reactive hydroxyl groups on the cellulose surface, with the induction of fairly strong shearing and compression forces. In this study, the mechanochemically activated WCF was used as a low cost but effective functional additive for the enhancement of the melt processability and mechanical properties of reclaimed PU foam. The influence of the WCF content on the composites' melt processability, mechanical properties, and dynamic mechanical properties is discussed in detail.

EXPERIMENTAL

Materials

The waste PU foam used in this study was derived from sole materials and was kindly provided by Jiangsu Meiah Rubber & Plastics Technology Co., Ltd. (Zhenjiang, China). It was smashed by an industrial crusher and used as such without any further purification. The obtained PU granules had an irregular shape with a particle size of 2–5 μm. The WCF used in this study was obtained commercially from the surplus of textile industries.

Mechanochemical Activation of the Cellulose Fibers

The mechanochemical activation of cellulose was achieved through high shearing and compression forces generated by the pan-mill-type mechanochemical reactor. The details of the pan-mill equipment and operation procedure can be found in our previous publications.[24,25] Generally, we obtained granules (5–10 mm in diameter) of the cotton cellulose fibers with easier access to the pan mill by chopping the pulp. After that, they were fed in a hopper set at the middle of the moving pan. The milled powder was discharged from the brim of the pans. The discharged powder was then collected for the next milling cycle. The whole milling process at ambient temperature was maintained at a rotating speed of 30 rpm and a specific pressure.

Preparation of the Thermoplastic PU/WCF Composites

By altering the content of WCF in the composites, we prepared four composites with PU/WCF weight ratios of 100/25, 100/50, 100/75, and 100/100, respectively. We prepared the blends in a Brabender Plasticorder PLE-330 (Duisburg, Germany) by melt mixing the components at a temperature of 180°C and a rotor speed of 30 rpm for 8 min. After that, all of the samples were molded on a MiniJet injection molding machine (Thermo Fisher Scientific, Karlsruhe, Germany) under a pressure of 10 MPa at 210°C for 5 min.

Morphological Observation

Scanning electron microscope (JEOL model JSM-5600, Tokyo, Japan) was used to observe the morphology of the cellulose fibers and the liquid-nitrogen-fractured surface of the composite samples. Before scanning electron microscopy (SEM) evaluation, the samples were sputter-coated with gold to prevent charging during the tests.

Size and Specific Surface Area Analysis

The average particle size and particle size distribution of the cellulose powder were measured by a Masterizer 2000 laser particle analyzer (Malvern, Britain). The range of size analysis was 0.3–100 μm. An appropriate amount of each sample was dispersed in the suspension medium (water) with a *p*-octyl poly(ethylene glycol) phenyl ether emulsifier as a dispersing agent and stirred at a pumping speed of 2400 rpm. We obtained more correct data by breaking up the flocculates ultrasonically. Then, the particle size and its distribution were calculated from the light-scattering pattern. The specific surface area of the WCF powder was estimated simultaneously.

Fourier Transform Infrared (FTIR) Analysis of Cellulose

FTIR spectroscopy was performed by means of a Nicolet 20SXB FTIR spectrometer (Madison, Wisconsin), with 32 scans taken for each sample at a resolution of 2 cm^{-1}, ranging from 400 to 4000 cm^{-1}. KBr pellets of the samples were prepared by the mixture of 2 mg of WCF powders with 200–300 mg of KBr in a carnelian mortar. The pellets (diameter = 1 cm) were prepared in a standard tool under a pressure of 4 MPa. Both the cellulose powders and KBr were dried before testing.

Wide-Angle X-ray Diffraction (WAXD) Analysis

WAXD measurements were performed in a Philips Analytical X'Pert X-diffractometer (Almelo, Netherlands) with Cu Kα radiation at $\lambda = 0.1540$ nm (40 kV and 40 mA). The measurements were conducted on powder compacted into small mats. WAXD data were collected at 2θ values from 5 to 50° with a step interval of 0.02°. The degree of crystallinity could be expressed relative to the crystallinity index (CrI). The equation used to calculate CrI was described by Segal et al.[26] in the following form:

$$\mathrm{CrI}\ (\%) = [(I_{002} - I_{\mathrm{am}})/I_{002}] \times 100$$

where I_{002} is the counter reading at the peak intensity at a 2θ angle close to 22° and represents the crystalline part and I_{am} is the counter reading at the peak intensity at a 2θ close to 18° and represents the amorphous part in cellulose.

Raman Analysis

Raman spectra were recorded on a Bruker Fourier transform Raman spectrometer VERTEX-70 (Bruker Optics, Ettlingen, Germany) with a diode-pumped Nd:YAG laser at an operating wavelength of 1064 nm. The measurements were performed with a 180° angle scattering geometry with 100 scans and a laser power of 500 mW at the sample location. Samples of the PU/WCF composites were obtained from injection molding. The interferograms were apodized with the Blackman–Harris four-term function and Fourier-transformed.

Tensile Tests

The stress–strain properties were measured according to ASTM D 412-80 with dumbbell test pieces with an Instron 5567 universal testing machine (Boston, Massachusetts) at a crosshead speed of 500 mm/min. Each sample was measured at least five times to eliminate experimental error. All of the tests were conducted at a room temperature of 23°C.

Heat-Shrinkage Measurements

Strips of the samples were taken for this experiment. The samples with and without pretreatment were prepared with a Haake MiniJet, (Karlsruhe, Germany) at 210°C. The samples were taken out and set aside for 24 h to allow any elastic rebound. From the length of the barbell mold and the sample, the heat shrinkage (%) was calculated as follows:[27]

$$\mathrm{Heatshrinkage}\ (\%) = (L - L_{\mathrm{o}})/L \times 100$$

where L is the length of the barbell mold and L_o is the length of the sample after shrinkage.

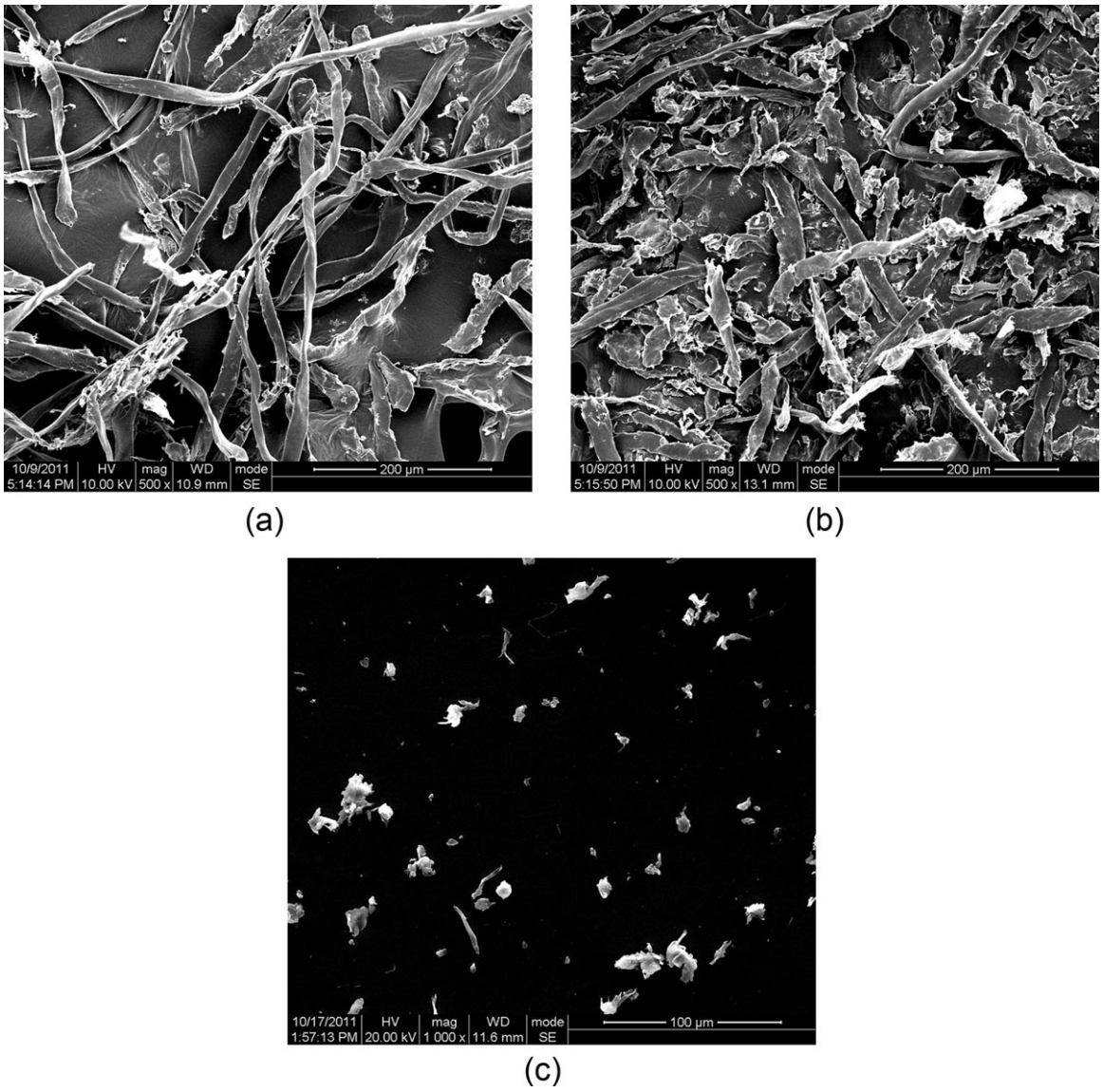

Figure 1. SEM images of the WCF powders (a) before and after (b) 5 and (c) 40 cycles of pan milling.

Dynamic Mechanical Analysis (DMA)

DMA was carried out on a dynamic mechanical thermal analyzer (TA Q800, New Castle, PA Pennsylvania) from Polymer Laboratory. The measurements were conducted under a tension mode with dimensions of 14 × 4 × 2 mm^3 and a heating rate of 5°C/min from −100 to 120°C at atmospheric pressure. The frequency was fixed at 1 Hz.

RESULTS AND DISCUSSION

Morphological Development of WCF During Pan Milling

The morphological development of WCF during pan milling was estimated by SEM observation. The SEM micrographs of the WCF powder before and after milling are shown in Figure 1. Figure 1(a) shows the SEM micrograph of the initial WCF powder, which consisted of comparatively tangled fibers and bundles with a smooth surface. Figure 1(b) shows the SEM micrograph of the WCF powder after 5 cycles of pan milling. The WCF fibers began to lose their fibrillar structure, and some with untangled structures were also obtained. Figure 1(c) shows the SEM micrograph of the WCF powder after 40 cycles of pan milling. The fibrous structure of WCF was completely destroyed, and a fine powder was obtained because of the effects of strong shearing and squeezing stresses during pan milling. At 40 cycles, for example [Figure 1(c)], the particle size of WCF became smaller and exhibited a more uniform and finer powder structure as the milling times were prolonged; this indicated that mechanochemical milling was an effective pretreatment method for reducing the particle size. A similar result was achieved in the research of Ghose.[28]

Size Reduction During Pan Milling and Specific Surface Area Analysis

To further investigate the effect of mechanochemical milling on the morphology of WCF, the average particle size and particle size distribution of the WCF powder were measured. The results are shown in Figure 2. Figure 2(a) shows the effect of pan milling on

Applied Polymer SCIENCE

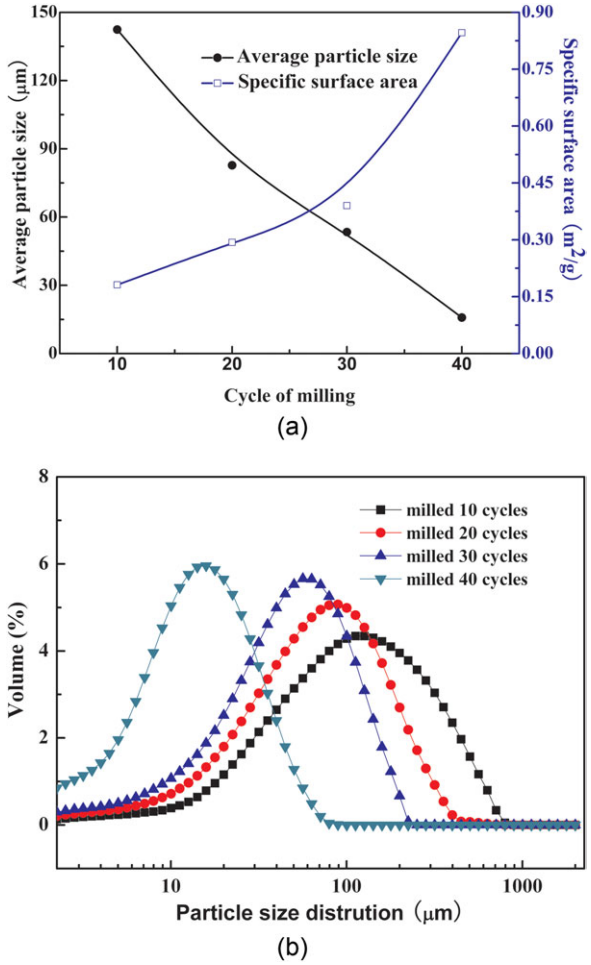

Figure 2. Effects of pan milling on the (a) particle size and specific surface area and (b) particle size distribution of WCF powders. [Color figure can be viewed in the online issue, which is available at wileyonlinelibrary.com.]

the particle size and specific surface area of WCF. The results indicate that the average particle size of the WCF powder decreased sharply with increasing milling time as a result of the pulverization of large particles. Meanwhile, the specific surface area increased with increasing milling time; this indicated that the separation and breakage of the WCF fibers into small particles produced a greater surface area at the cut edges.

The effect of pan milling on the particle size distribution of WCF is shown in Figure 2(b). The particle size of the WCF powder moved to a smaller diameter with increasing milling time. The average volume of the mean diameter was 63 μm after 10 cycles of milling. After 40 cycles of milling, the average particle size decreased to 15.8 μm, and the particle size distribution curve became the widest of four samples because of the generation of some smaller particles.

FTIR Analysis of Cellulose

FTIR spectroscopy is a useful tool for obtaining rapid information about the structure of cellulose and the chemical changes that take place in cellulose because of various treatments. The spectra of the WCF powder before and after 40 cycles of milling are shown in Figure 3. The absorption peak around 1060 cm^{-1} was ascribed to —C—O— stretching vibrations, which are the symbol of a glucose ring. The intensity of this peak was not changed after pan milling; this demonstrated that the mechanochemical degradation of cellulose could have hardly occurred at glucose rings. No new absorption peaks arose after milling; this illustrated that no other functional groups were generated during milling. A similar result was reported by Staudinger and Dreher,[29] who treated cellulose from spruce by ball milling. The broad and strong peak ranging from 3200 to 3600 cm^{-1} and assigned to —OH groups showed a marked increase after mechanochemical pretreatment and was ascribed to the intramolecular and intermolecular hydrogen bonds of cellulose.[30] Schwanninger et al.[31] reported that the O—H stretching vibration region became broader during mechanical milling because of the breakage of the hydrogen bonds of cellulose. The broadening of the peak at 3412 cm^{-1}, which was ascribed to O—H stretching vibration after pan milling, is shown in Figure 3; this accorded well with this view.

WAXD Analysis of Cellulose

To investigate the crystalline structural changes of the WCF cellulose, WAXD analysis was conducted. Figure 4 shows the WAXD patterns of the WCF cellulose before and after 20 cycles of pan milling. The results indicate that intensive mechanical action on the polymers was able to cause damage to the macromolecular chains and led to the mutual displacement of separate structural units. The displacement of structural elements of the polymeric chains was first accompanied by the distortion of the initial packing of the chains and a loss of ordering. The sharp, high diffraction peak of the WCF cellulose appeared at a 2θ value close to 22° and was assigned to the (002) lattice plane of cellulose I.[32,33] The two overlapping flatter diffractions at a 2θ value close to 15° were assigned to the (101) and ($10\bar{1}$) lattice planes of cellulose I.[34] The most significant change was the weakening of the diffraction peak intensity, which indicated that the crystalline ordered scattering units were sharply reduced because of a breakage of the original crystallites and a considerable rupture of the intermolecular hydrogen bonds. Vittadini et al.[35] reported that the amorphous part of cellulose was more readily accessible by reactants and had more activation. Thus, a decrease in the crystallinity of WCF after mechanochemical pretreatment benefitted its interfacial adhesion with the polymer matrix.

Raman Analysis of the PU/WCF Composites

Raman analysis is an important method for studying the structural changes of hydrogen bonds. Raman shifting can provide an insight on the interfacial interaction between the fillers and PU matrix. To investigate the changes in the intramolecular and intermolecular hydrogen bonds of the PU/WCF composites, we conducted Raman spectroscopy. Figure 5 shows the partial Raman spectra of the PU and PU/WCF composites. In general, the variation of the Raman scattering intensities of the urethane functional groups (N—H stretching, amide I at about 1732 cm^{-1}, amide II at about 1530 cm^{-1}, and amide III at about 1303 cm^{-1})[36] could be used to investigate the hydrogen bonds of PU. Strong peaks in this spectral range of about 1000–2000 cm^{-1} appeared in the Raman spectra of the pure PU and PU/unpretreated WCF composites; this indicated the existence of

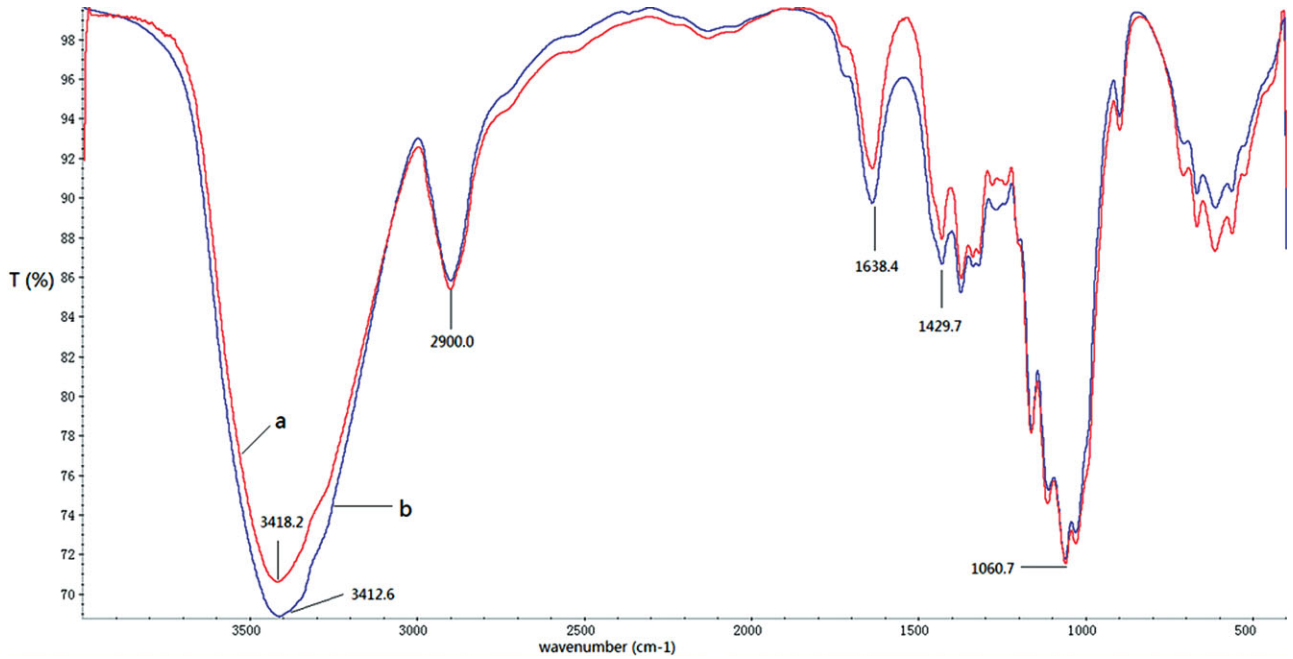

Figure 3. FTIR spectra of the WCF cellulose before and after 40 cycles of pan milling. [Color figure can be viewed in the online issue, which is available at wileyonlinelibrary.com.]

abundant exposed N—H groups. It was interesting to note that with the addition of mechanochemically activated WCF, the Raman peaks of the PU/WCF composites in this spectral range weakened and almost disappeared. The results indicate that the free hydroxyl groups exposed on the WCF surface could establish new hydrogen bonds with the N—H groups of the PU molecules; this led to the significant weakening of the Raman peaks of N—H groups.

Mechanical Properties of the Thermoplastic PU/WCF Composites

The ultrafine pulverization and hydrogen-bond breakage of WCF due to the mechanochemical pretreatment could have also influenced its adhesion ability to the reclaimed PU matrix and, thus, altered the mechanical properties of the PU/WCF composites. The effect of the mechanochemical pretreatment on the elongation at break of the PU/WCF composites is shown in Figure 6. It was apparent that the elongation at break values of the composites prepared from the mechanochemically activated WCF were much better than those of the untreated WCF, and this effect became more evident with increasing WCF content. With the addition of more than 50-phr untreated WCF to the composites, the elongation at break sharply decreased to lower than 2.3%. This result limits its application as a thermoplastic elastomer. On the other hand, with the addition of the 50-phr mechanochemically activated WCF to the PU matrix, the elongation at break values of the PU/WCF composites were even

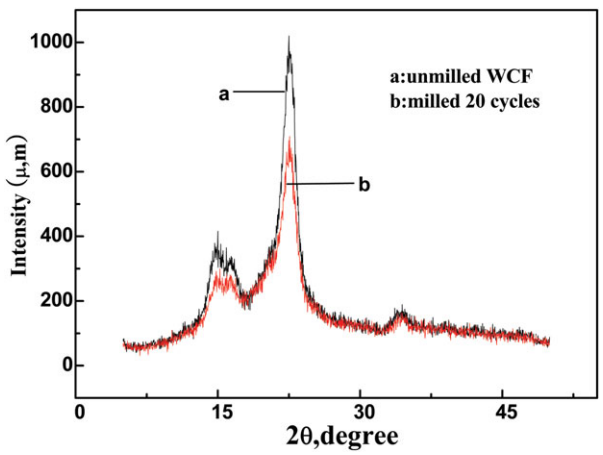

Figure 4. WAXD patterns of the WCF cellulose before and after 20 cycles of pan milling. [Color figure can be viewed in the online issue, which is available at wileyonlinelibrary.com.]

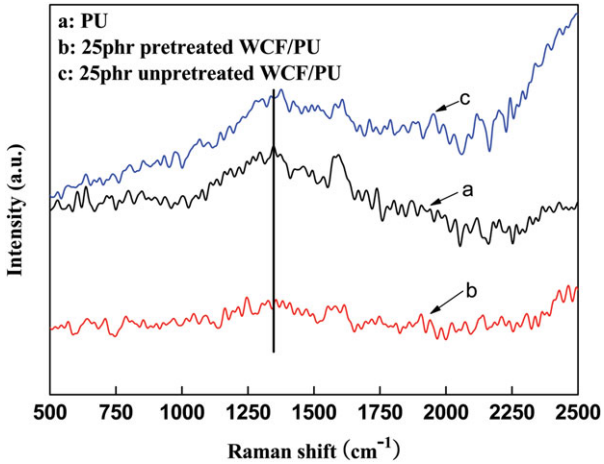

Figure 5. Raman spectra of the pure PU and PU/WCF composites. [Color figure can be viewed in the online issue, which is available at wileyonlinelibrary.com.]

Applied Polymer SCIENCE

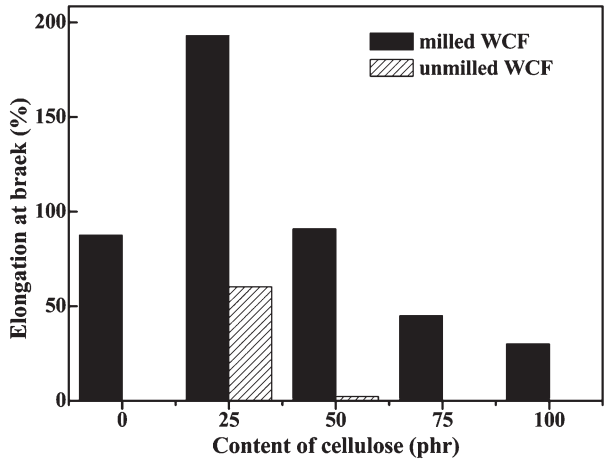

Figure 6. Effect of the mechanochemical pretreatment on the elongation at break of PU/WCF composites with various WCF contents.

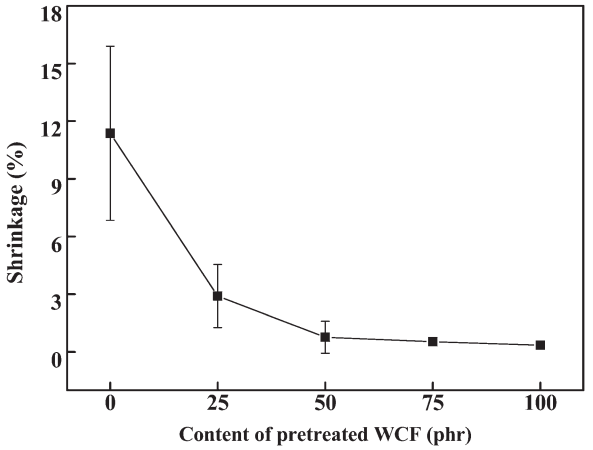

Figure 8. Effect of the pretreated WCF content on the heat shrinkage of the PU/WCF composites.

higher than that of the pure PU matrix. The enhancement of the elongation at break through the mechanochemical pretreatment of WCF could be ascribed to the improved interfacial adhesion between the activated WCF and PU matrix. In view of the poor mechanical properties of the untreated WCF-filled composites, the mechanochemically activated WCF was used for the preparation of all of the PU/WCF composite samples in this study.

The effects of the pretreated WCF content on the tensile strength and Young's modulus values of the PU/WCF composites are shown in Figure 7. The tensile strength of the PU/WCF composites increased with increasing pretreated WCF content. With the addition of 75-phr pretreated WCF to the PU matrix, the tensile strength increased from its original 10.3 to 23.2 MPa, an enhancement of 125.2%; meanwhile, the Young's modulus increased from its original 31.8 to 664.6 MPa, an increase of over 20 times. This was attributed to the good interfacial bonding between the pretreated celluloses and the PU matrix, which facilitated effective stress transfer. The results demonstrate that the mechanochemically activated WCF was low in cost but was an efficient reinforcing filler for the PU matrix. The reinforcing effect of cellulose was consistent with the results of other researchers.[37–39]

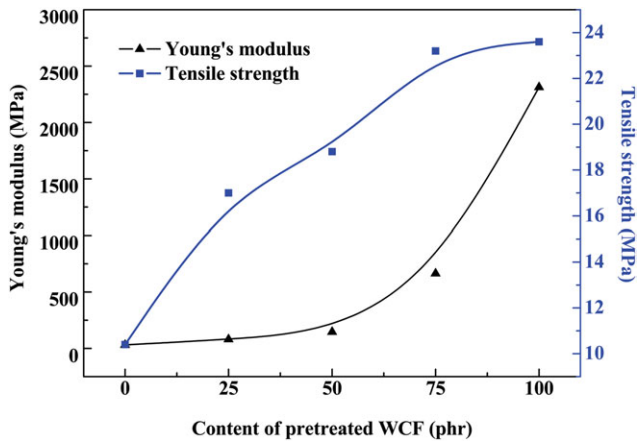

Figure 7. Effects of the pretreated WCF content on the tensile strength and Young's modulus values of the PU/WCF composites. [Color figure can be viewed in the online issue, which is available at wileyonlinelibrary.com.]

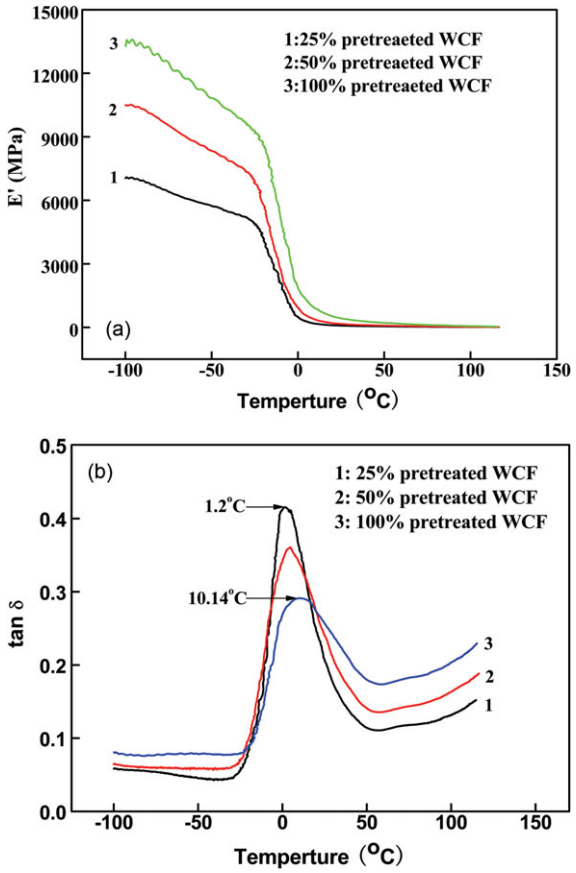

Figure 9. (a) E' and (b) tan δ versus temperature curves of the PU/WCF composites with various WCF contents. [Color figure can be viewed in the online issue, which is available at wileyonlinelibrary.com.]

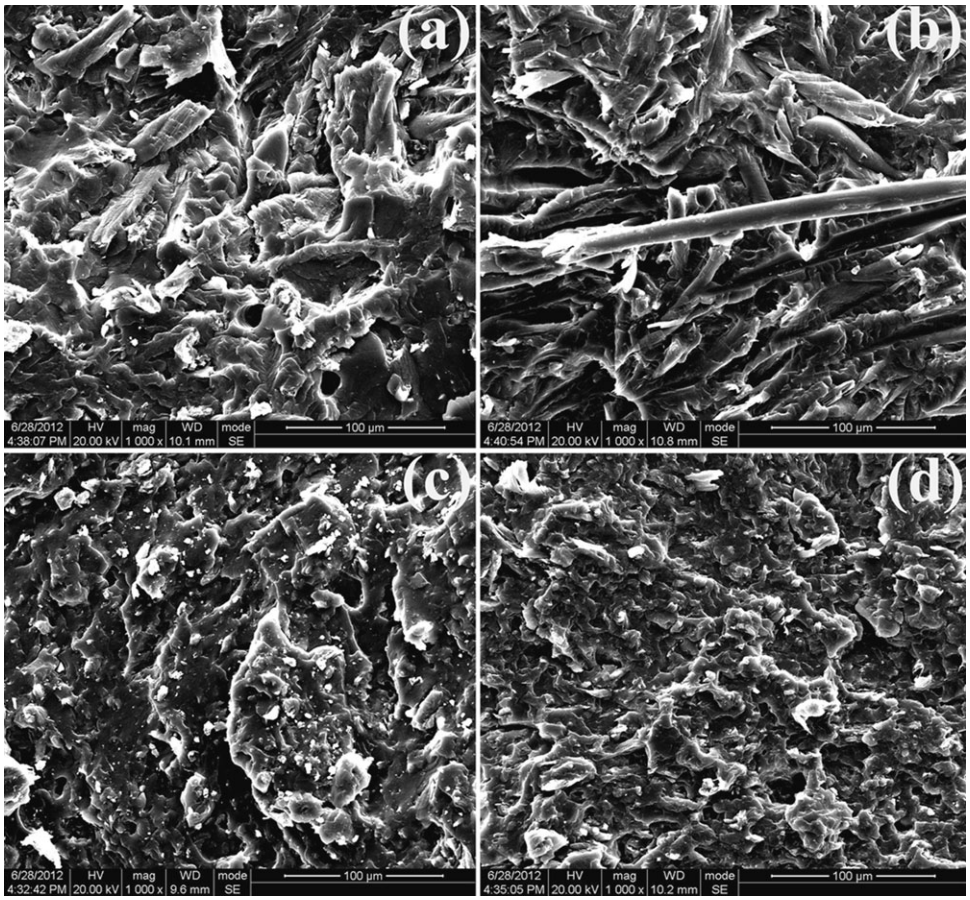

Figure 10. SEM photographs of the PU/WCF composites filled with (a) 25-phr unpretreated WCF, (b) 50-phr unpretreated WCF, (c) 25-phr activated WCF, and (d) 50-phr activated WCF, respectively.

Heat Shrinkage of the Thermoplastic PU/WCF Composites

The PU matrix used in this study was reclaimed PU foam and was derived from the shoe manufacturing industry. It had poor melt processability, and it was difficult to obtain its integrated sample. To investigate the effect of the pretreated WCF content on the melt processability of the PU/WCF composites, the heat-shrinkage value was measured and is shown in Figure 8. The heat-shrinkage value sharply decreased with increasing pretreated WCF content. With the addition of more than 50-phr pretreated WCF to the composites, almost no heat shrinkage was observed. Meanwhile, the error range of the PU/WCF composites decreased with increasing WCF content; this further confirmed the enhancement in melt processability. The results indicate that the mechanochemically activated WCF could be used as a functional filler to enhance the melt processability of reclaimed PU foam. The fairly strong shearing and compression forces exerted by the pan-mill equipment destroyed the hydrogen bonds and released reactive hydroxyl groups, which established a new hydrogen-bond network with PU molecules.[40] As a result, the interfacial adhesion between the pretreated WCF and the PU matrix was improved. The rigid WCF effectively restricted the heat shrinkage of the PU matrix. Furthermore, the small particle size of the cellulose powder displayed excellent morphological stability and dispersability against shrinking because of the steric effect of the composites.

DMA

DMA is a useful technique that is commonly used to characterize the time and temperature dependency of the viscoelastic nature of polymers. The ratio of the loss modulus (energy lost as viscous dissipation) and storage modulus (E'; elastic energy stored during deformation) is known as tan δ and indicates the damping characteristic of materials.

The dynamic mechanical parameters (E' and tan δ) for the blend composites are plotted as a function of temperature at a constant frequency of 1 Hz (Figure 9). The E' values of the PU/WCF composites increased with increasing pretreated WCF content, as shown in Figure 9(a); this corresponded well with the mechanical properties results. The tan δ versus temperature curves are shown in Figure 9(b). The tan δ peak was associated with the glass transition of the PU molecules. The glass-transition temperature, which represents one of the major viscoelastic transitions of a material, is often obtained from the maximum of the tan δ curve.[41] The glass-transition temperature of the PU moved to higher temperatures with increasing pretreated WCF content; this was attributed to the hindered cooperative motion of the polymer chains. This result indicated that strong interfacial interaction between the pretreated WCF and PU matrix was realized. The same phenomenon has been observed in other fiber-reinforced elastomer composites.[42,43]

Morphological Observation on the Fractured Surface of the PU/WCF Composites

Figure 10(a, b) shows the SEM images of the liquid-nitrogen-fractured surfaces of the PU composites filled with 25- and 50-phr unpretreated WCF, respectively. A clear interface could be seen in the PU/unpretreated composites; this indicated the poor adhesion between the two phases. In contrast, the interface of the PU composites filled with 25- and 50-phr pretreated WCF were vague and made it difficult to distinguish the two phases. The mechanochemically activated WCF was well coated and firmly embedded in the PU matrix because of its large specific surface area and increased interfacial interaction. This was consistent with the results of Raman spectroscopy described earlier and indicated the strong hydrogen-bonding interactions between the mechanochemically activated WCF and the PU matrix.

CONCLUSIONS

An activated WCF ultrafine powder was successfully prepared through a mechanochemical route and was used as a reinforcement to enhance the melt processability and mechanical properties of reclaimed PU foam. The following conclusions were drawn:

1. The fairly strong shearing and compression forces exerted by the pan mill destroyed the hydrogen bonds of the WCF cellulose and released reactive hydroxyl groups, which were beneficial to the interfacial interaction between the WCF and PU matrix.
2. The mechanical properties of the PU/WCF composites were significantly improved through the mechanochemical pretreatment of WCF. This was ascribed to the improved interfacial adhesion between the WCF and PU matrix, as confirmed by the DMA results.
3. Mechanochemically activated WCF powder could be used as a low-cost but effective functional filler to enhance the melt processability of reclaimed PU foam. The heat shrinkage of the composites sharply decreased with increasing pretreated WCF content.

ACKNOWLEDGMENT

The authors thank the National Science Foundation of China (contract grant numbers 51203105 and 51073108) and National High Technology Research and Development Program (863 Program, contract grant number SS2012AA062613) for financial support.

REFERENCES

1. Hilmar, K.; John, J. K.; Richard, A. V. *Macromolecules* **2008**, *41*, 4709.
2. Poomali, S.; Sureshac, B.; Joong-Hee, L. *Mater. Sci. Eng. A* **2008**, *492*, 486.
3. Becker, D.; Roeder, J.; Oliveira, R. V. B.; Soldi, V.; Pires, A. T. N. *Polym. Test.* **2003**, *22*, 225.
4. Gadea, J.; Rodríguez, A.; Campos, P. L.; Garabito, J. *Cement Concrete Compos.* **2010**, *32*, 672.
5. Kumar, C. R.; Karger-Kocsis, J. *Eur. Polym. J.* **2002**, *38*, 2231.
6. Benes, H.; Rosner, J.; Holler, P.; Synkova, H.; Kotek, J.; Horak, Z. *Polym. Adv. Technol.* **2007**, *18*, 149.
7. Watando, H.; Saya, S.; Fukaya, T.; Fujieda, S.; Yamamoto, M. *Polym. Degrad. Stab.* **2006**, *91*, 3354.
8. Asahi, N.; Sakai, K.; Kumagai, N.; Nakanishi, T.; Hata, K.; Katoh, S.; Moriyoshi, T. *Polym. Degrad. Stab.* **2004**, *86*, 147.
9. Matsumiya, Y.; Murata, N.; Tanabe, E.; Kubota, K.; Kubo, M. *J. Appl. Microbiol.* **2010**, *108*, 1946.
10. Im, E. J.; Kim, S. H.; Lee, K. H. *J. Anal. Appl. Pyrolysis* **2008**, *82*, 184.
11. Miranda, R.; Sosa-Blanco, C.; Bustos-Martinez, D.; Vasile, C. *J. Anal. Appl. Pyrolysis* **2007**, *80*, 489.
12. Zhang, X.; Yang, H.; Yang, T.; Lin, Z.; Tan, S. *J. Appl. Polym. Sci.* **2012**, *123*, 562.
13. Tserki, V.; Matzinos, P.; Panayiotou, C. *J. Appl. Polym. Sci.* **2003**, *88*, 1825.
14. Xiong, R.; Zhang, X. X.; Tian, D.; Zhou, Z. H.; Lu, C. H. *Cellulose* **2012**, *4*, 1189.
15. Usarat, R.; Duangduen, A.; Duangdao, A. O. *Carbohydr. Polym.* **2012**, *87*, 84.
16. Zhang, X. X.; Lu, C. H.; Liang, M. *J. Appl. Polym. Sci.* **2007**, *103*, 4087.
17. Zhang, X. X.; Lu, C. H.; Liang, M. *Plast. Rubber Compos.* **2007**, *36*, 370.
18. Zhang, X. X.; Lu, C. H.; Liang, M. *J. Polym. Res.* **2009**, *16*, 411.
19. Zhang, X. X.; Lu, C. H.; Liang, M. *J. Appl. Polym. Sci.* **2011**, *122*, 2110.
20. Zhang, X. X.; Lu, C. H.; Zheng, Q. Y.; Liang, M. *Polym. Adv. Technol.* **2011**, *22*, 2104.
21. Zhang, X. X.; Chen, C.; Lu, C. H. *Prog. Rubber Plast. Recycl. Technol.* **2012**, *28*, 81.
22. Zhang, X. X.; Lu, Z. X.; Tian, D.; Li, H.; Lu, C. H. *J. Appl. Polym. Sci. [Online early access]*. DOI: 10.1002/APP.37721. Published online May 24, **2012**. http://onlinelibrary.wiley.com/doi/10.1002/app.37721/full.
23. Shao, W. G.; Wang, Q.; Wang, F.; Cheng, Y. H. *Carbon* **2006**, *44*, 2708.
24. Zhang, W.; Lu, C. H.; Liang, M. *Cellulose* **2007**, *14*, 447.
25. Zhang, W.; Yang, X. L.; Li, C. Y.; Liang, M.; Lu, C. H.; Deng, Y. L. *Carbohydr. Polym.* **2011**, *83*, 257.
26. Segal, L.; Creely, J. J.; Martin, A. E.; Conrad, C. M. *Text. Res. J.* **1959**, *29*, 786.
27. Sujit, K. D.; Chati, T. K.; Tikku, V. K.; Pradhan, N. K.; Bhowmick, A. K. *Radiat. Phys. Chem.* **1997**, *50*, 399.
28. Ghose, T. K. *Biotechnol. Bioeng.* **1969**, *11*, 239.
29. Staudinger, H.; Dreher, E. *Ber. Dtsch. Chem. Ges.* **1936**, *69*, 1091.
30. Romeu, C.; Ludmila, C. F.; Camila, M. L.; Thomas, H.; Omar, A. E. *Carbohydr. Polym.* **2011**, *83*, 1285.

31. Schwanninger, M.; Rodrigues, J. C.; Pereira, H.; Hinterstoisser, B. *Vib. Spectrosc.* **2004**, *36*, 23.

32. Prachayawarakorn, J.; Ruttanabus, P.; Boonsom, P. *J. Polym. Environ.* **2011**, *19*, 274.

33. Mariko, A.; Takashi, E.; Takahiro, H. *Cellulose* **2004**, *11*, 163.

34. Heritage, K. J.; Mann, J.; Roldan-Gonzalez, L. *J. Appl. Polym. Sci.* **1963**, *1*, 671.

35. Vittadini, E.; Dickinson, L. C.; Chinachoti, P. C. *Carbohydr. Polym.* **2001**, *46*, 49.

36. Parnell, S.; Min, K.; Cakmak, M. *Polymer* **2003**, *44*, 5137.

37. Nadhan, A. V.; Rajulu, A. V.; Li, R.; Jie, C.; Zhang, L. *J. Polym. Environ.* **2012**, *20*, 454.

38. Zou, Y.; Narendra, R.; Yang, Y. Q. *Compos. B* **2011**, *42*, 763.

39. Jawaid, M.; Abdul, K. H. *Carbohydr. Polym.* **2011**, *86*, 1.

40. Lu, Q. W.; Christopher, W. M. *Polymer 2004*, *45*, **1981**.

41. Quan, H.; Zhang, B. Q.; Zhao, Q.; Richrad, K. Y.; Robert, K. Y. L. *Compos. A* **2009**, *40*, 1506.

42. Joy, K. M.; Kim, I. I.; Chang-Sik, H. *Macromol. Rapid Commun.* **2003**, *24*, 671.

43. Madjid, F. F.; Seyed, H. J.; Hossei, A. K.; Ahmad, Y.; Raheleh, B.; Mohammad, T. *Macromol. Mater. Eng.* **2007**, *292*, 1103.